

Article

ENSO Impact on Summer Precipitation and Moisture Fluxes over the Mexican Altiplano

José P. Vega-Camarena ¹, Luis Brito-Castillo ^{1,*}, Luis F. Pineda-Martínez ² and Luis M. Farfán ³

¹ Centro de Investigaciones Biológicas del Noroeste (CIBNOR), Guaymas 85454, Mexico; jcamarena006@gmail.com

² Unidad de Ciencias Sociales, Universidad Autónoma de Zacatecas, Zacatecas 98066, Mexico; lpineda@uaz.edu.mx

³ Centro de Investigación Científica y de Educación Superior de Ensenada (CICESE), La Paz 23050, Mexico; farfan@cicese.edu.mx

* Correspondence: lbrito04@cibnor.mx; Tel.: +52-622-22-122-37

Abstract: In the warm season, El Niño/Southern Oscillation (ENSO) causes periods with more rain in Northern Mexico during its positive phase, while less rainfall is recorded in the southern regions during the negative phase. This research study evaluates the variability of summer (July–September) precipitation and moisture fluxes under different ENSO scenarios in the Mexican Altiplano and coast of the state of Nayarit. The catchment of Rio San Pedro-Mezquital (SPM-RB) connects both regions. Using the Oceanic Niño Index (ONI), the years that signal change from El Niño to La Niña (1998), neutral conditions (2005), and strong (moderate) La Niña (1999) were selected to get an insight of ENSO impact on summer precipitation. For anomalies in the Altiplano, two additional contrasting years were analyzed—2006 (mostly dry) and 2010 (wet)—to determine moisture sources. Summer rainfall conditions in 1998 and 1999 had an opposite behavior between coastal Nayarit (wet) and the Altiplano (dry), while in 2005, rainfall deficits were observed in both regions. The moisture fluxes showed large divergence areas over central Mexico and the Southeastern United States in years of intense drought (1998 and 1999) caused by two high-pressure cells at middle levels of the troposphere (500 hPa). The moisture transport mechanisms into the Altiplano were related to atmospheric circulation at the upper level (200 hPa). The variations of the moisture fluxes from 2006 to 2010 are less strong at middle levels. The Eastern Pacific moisture convergence along the western coast of Mexico favors above-average rainfall anomalies in the coastal region but below-average anomalies in the Altiplano.

Keywords: Mexican Altiplano; rainfall anomalies; moisture fluxes; weather research and forecasting model; North American monsoon



Citation: Vega-Camarena, J.P.; Brito-Castillo, L.; Pineda-Martínez, L.F.; Farfán, L.M. ENSO Impact on Summer Precipitation and Moisture Fluxes over the Mexican Altiplano. *J. Mar. Sci. Eng.* **2023**, *11*, 1083. <https://doi.org/10.3390/jmse11051083>

Academic Editor: Jean-Louis Pinault

Received: 17 April 2023

Revised: 10 May 2023

Accepted: 19 May 2023

Published: 20 May 2023



Copyright: © 2023 by the authors. Licensee MDPI, Basel, Switzerland. This article is an open access article distributed under the terms and conditions of the Creative Commons Attribution (CC BY) license (<https://creativecommons.org/licenses/by/4.0/>).

1. Introduction

Knowledge of the mechanisms that affect the climate in Mexico has increased at different scales from interannual to decadal variability [1–4]. In particular, previous works [1,5,6] have described distinct mechanisms that control the spatial and temporal precipitation distribution. The subtle changes in the position and strength of the subtropical, high-pressure systems of the Eastern Pacific and North Atlantic have been related to the conditions of sea surface temperature (SST) in the tropical Pacific, for instance, El Niño/Southern Oscillation (ENSO), which modifies the precipitation patterns in Mexico [6–10].

Under the positive phase of ENSO conditions, summers are rainy in Northern Mexico and drier towards the south [6,11]. Unfortunately, the connection between ENSO and summer precipitation is not simply linear. Many studies have failed to identify a consistent relationship [4,11–13]. For instance, [13] summer precipitation may be enhanced following winter/spring El Niño events related to intense tropical storm activity and moisture flow over Northwestern Mexico. Zolotokrylin et al. [14] examined the impact of ENSO events

on generating wet and dry conditions in the Sonoran Desert. Cid-Serrano et al. [15] defined an ENSO-index to measure its relationship to rainfalls in the Latin American Pacific coasts. Other works [4,16] have found that summers are wet in Mexico during the positive phase of ENSO (i.e., El Niño) years and the cold phase of monthly SST in the North Pacific (i.e., the Pacific Decadal Oscillation or PDO). More recently, Wang et al. [17] found that when ENSO and PDO are out of phase, dry-wet variations over the global land distribution weaken or even disappear. In general, the negative phase of ENSO (i.e., La Niña phase) produces opposite conditions to those observed during the El Niño years. For instance, the droughts of 1890 and the first half of the 1950s in northern Mexico [18] probably occurred in response to multi-year effects of La Niña [12].

La Niña conditions, in combination with the cold phase of the PDO and warm phase of the Atlantic Multidecadal Oscillation (AMO), are more effective in producing intense droughts in the Mexican Altiplano [3,12,19]. Because this combination is associated with moisture flows from the tropical Southeastern to Northern Mexico regions that are weaker than normal, they also cause a reduction in the number of hurricanes in the Pacific [20]. Other combinations, such as La Niña and similar phases in PDO and AMO or the transition from El Niño to La Niña or La Niña to El Niño, can produce weak or moderate drought conditions in the Altiplano [19]. However, the role of the El Niño effect on the advection of moisture fluxes, particularly in the region of the San Pedro-Mezquital River Basin (SPM-RB), which connects the coast with the Altiplano, still remains unclear. The region off and along the coast of Nayarit is very prolific in the development of mesoscale convective systems (MCS) [21] that can move across the Gulf of California, cause heavy rainfall and lightning activity, and are part of the region's warm-season climatology. The scientific interest in this research is based on the MCSs causing a lag in the warm season progression of the month of maximum precipitation in Western Mexico [22,23].

Previous works have shown evidence about the existence of teleconnection between the SST anomalies in the Eastern Pacific and precipitation in Mexico [6,8]. Additionally, Farfán et al. [21] identified a persistent deep convection region along and off the coast of Nayarit, while another study [23] showed that summer rainfall behaves in a contrasting way along coastal Nayarit to that observed on the Mexican Altiplano. It is important to note that this region is positioned in the transition zone where the annual precipitation cycle changes from the double precipitation peak with the midsummer drought to the south, to a single rainfall peak characteristic of the monsoon in the north [24]. All these features are important to understand seasonal and interannual precipitation variabilities in Western Mexico. According to Vega-Camarena et al. [23], under certain conditions, a see-saw rainfall pattern is observed between the coast and Altiplano, i.e., dry in the Altiplano and wet in the coast of Nayarit, and vice versa. Since the Altiplano region is flanked by the Sierra Madre Occidental to the west and Sierra Madre Oriental to the east, the two mountain massifs act as barriers that prevent the entry of moisture from the Pacific and Gulf of Mexico into this region, causing its arid conditions. Therefore, it is of great interest to understand the moisture flow pattern that contributes to rainfall in the Altiplano.

Moreover, the study of ENSO impact over summer precipitation is crucial to elucidate the wet-dry changes that may affect the national economy, mainly drought [19], specifically concerning ENSO influence over summer precipitation in the highlands and area near the coast of Nayarit. The weather research and forecasting model (WRF) was implemented to verify the hypothesis that the atmospheric response on the Altiplano changes under different ENSO conditions by strengthening or weakening convective activity and rainfall production. In the next section, the selection of ENSO years used in this study, sources of data, and the WRF model configurations are set out. Then, the main results are described, and the implications of ENSO in the development of wet-dry conditions over the study region are discussed. Finally, concluding remarks are provided in the last section.

2. Materials and Methods

2.1. Description of the Study Area

The Mexican Altiplano is a high plain area located between two mountain ranges, the Sierra Madre Occidental (SMOc) to the west and Sierra Madre Oriental (SMOr) to the east (Figure 1). These mountain ranges act as a barrier that prevents moisture fluxes from the Pacific and Gulf of Mexico, which cause the predominantly arid climate in this region, mainly towards the north and northeast. In the upper portion of the SMOc, the climate is temperate and subhumid, and to the south, it is warm and sub-humid in coastal Nayarit and Jalisco. The average annual temperature varies from 17 °C in the northern states of Durango and Zacatecas to 25 °C in the southern coasts of Sinaloa and Nayarit. A precipitation gradient is observed between the Altiplano and the coast that varies from about 500 mm per year in the Altiplano to 800 mm in the SPM-RB and up to 1000 mm in the coast, with summer rainfall in the whole area driven by a monsoonal circulation system [2,5,25].

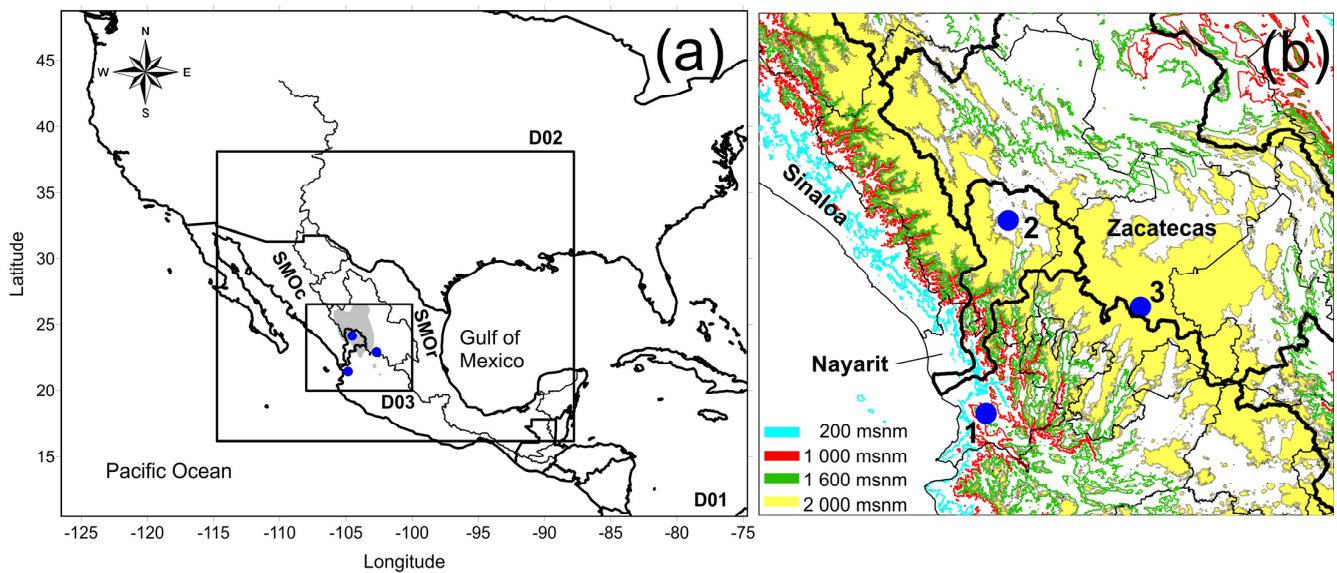


Figure 1. (a) Configuration of three domains (D01, D02, and D03) used in the weather research and forecasting (WRF) simulations; (b) topographic map showing 200 m, 1000 m, 1600 m and 2000 m contour levels in the D03 domain. In (a) the horizontal resolutions are 45 km (D01), 15 km (D02), and 5 km (D03), which cover the Mexican Altiplano (shaded area). Dots indicate station positions whose observations were used to validate the WRF model. The small polygon indicates the San Pedro-Mezquital River Basin (SPM-RB) in D03. The curves crossing from Northwestern to Southwestern Mexico show the continental divide. SMOc: Sierra Madre Occidental and SMOr: Sierra Madre Oriental. In (b) The thin black lines are outlines of Mexican states. Numbers correspond to station characteristics in Table 1.

Table 1. R²-YR and RMSE-YR values for observed hourly data and the WRF model for relative humidity and temperature.

No	Station Name, Year	R ² RH98	RMSE98	R ² T98	RMSE98	R ² RH05	RMSE05	R ² T05	RMSE05	Elevation, m
1	Tepic	0.56	11.1	0.73	2.10	0.55	11.18	0.57	2.80	963
2	Durango	ND	ND	0.80	2.49	0.60	16.93	0.75	2.85	1 871
3	Zacatecas	0.60	6.01	0.77	2.40	0.55	14.51	0.77	2.71	2 615

R² = the variance; YR = year; RMSE-YR = Mean square error-year; WRF = Weather Research and Forecasting model.

The San-Pedro Mezquital River Basin (SPM-RB), connects the Altiplano and coastal Nayarit through its canyon system. An outstanding characteristic of the SPM-RB is that the basin divide makes a large excursion inland (Figure 1), away from the coast and the

bulk of the SMOc massif. As such, the elevation for the basin and continental divide is quite a bit lower (i.e., closer to 2000 m) than it is in other regions of the SMOc. The displacement of the divide combined with a relatively low elevation appears to permit significant penetration of moisture into the continental interior, as it has been discussed [22] and further explored [19,23]. Additionally, it appears that the San-Pedro Mezquital Canyon System helps drive the anomalous increase in rainfall across latitudes limited to Nayarit.

2.2. Climate Data

Daily observations from the database of the National Meteorological Service of Mexico with a base period from 1970 to 2018 [26] were used to calculate the summer rainfall anomalies (July–September, JAS) of the years 1998, 1999, 2005, 2006 and 2010. In addition, hourly data (courtesy of the National Meteorological Service, Mexico) were used to evaluate the WRF outputs for temperature and relative humidity. The records were analyzed by calculating the R^2 and RMSE. The validation consisted of contrasting the hourly values of the observed and estimated relative humidity and temperature for the period from July to September 1998 and 2005. The results of the WRF simulation were compared with observations at three stations in Durango, Zacatecas, and Tepic (see Figure 1, Table 1).

2.3. The Weather Research Forecasting Model

Mesoscale meteorological models have become useful tools for short-term prediction [27–29]. The weather research and forecasting (WRF) version 4 “<https://esrl.noaa.gov/gsd/wrfportal/> (accessed on 10 January 2023)” is a mesoscale numerical model designed for weather forecasting operational and atmosphere research [30]. It has two dynamic cores, a data assimilation system and software architecture that facilitate the parallel calculation and extensibility of the system. The model serves a wide range of meteorological applications through scales from tens of meters to thousands of kilometers.

2.4. Model Setup

The WRF was established with the North American Regional Reanalysis (NARR) as the initial condition every 6 h <https://www.esrl.noaa.gov/psd/data> (accessed on 12 January 2023)”. NARR is a regional mesoscale analysis developed with a fixed boundary model and a data assimilation system [31,32]. For all model simulations, 3 domains and 30 vertical levels (Figure 1) were established. Domain 1 is in a grid of 83×84 nodes with a resolution of 45 km that covers North America, extending to the Pacific and Gulf of Mexico. Another domain had a grid of 151×151 nodes and 15 km resolution that covers the Southwestern United States and Mexico. A third, inner domain was centered in the SPM-RB with a grid of 109×97 points and 5 km resolution that embraces the Altiplano and the main Mexican region of rain-fed bean production [33]. For the WRF simulations, we used the parameterizations of CAM 5.1 5-class Scheme and WSM 3-Class Simple Ice Scheme in microphysics, RRTM scheme for longwave radiation, and Dudhia scheme for shortwave radiation, surface layer, MM5 scheme, and Unified Noah scheme for the land surface model. Other configurations were YSU for the planet’s boundary layer and physics Kain-Fritsch (new Eta) scheme for cumulus parameterization. This configuration of the model was the result of an experimental analysis tuning in test runs.

The Oceanic Niño Index (ONI) was used to select years with different ENSO-related conditions (see below). The NOAA Climate Prediction Center <https://www.cpc.ncep.noaa.gov/> (accessed on 13 February 2023) provides ONI, which is a three-month running mean of SST anomalies in El Niño 3.4 region (5°S – 5°N , 120°W – 170°W) relative to the 1971–2000 base period.

Based on the knowledge already generated on the effects of ENSO in Mexico in general (i.e., [9,12,34]) and in the Altiplano region in particular [19], some questions are still to be answered, such as what is the moisture flow related to rainfall in the Altiplano and how is rainfall variability in the Altiplano under different ENSO scenarios? Average anomaly rainfall maps were plotted during ENSO-related conditions, i.e., El Niño (1982, 1987, 1997),

La Niña (1971, 1974, 2011), neutral (1979, 1980, 1993), a transition from La Niña to El Niño (1976, 2009) and from El Niño to La Niña (1973, 1983) (Figure 2). According to Figure 2, the most interesting scenario is when the Altiplano is rainy, and the coast of Nayarit is dry, as it occurs during the transition from La Niña to El Niño events (Figure 2d). In the other cases, both regions are wet, as occurs during the transition from El Niño to La Niña event (Figure 2e) or both are dry, as occurs during El Niño years (Figure 2a), or wet in Nayarit and dry in the Altiplano, as occurs during neutral (Figure 2b) and La Niña (Figure 2c) years. It is clear, then, that to elucidate the moisture flow that generates rainfall in the Altiplano, the ENSO years that resulted in rainy conditions in the Altiplano should be investigated and the associated atmospheric circulation analyzed (i.e., during transition years, Figure 2d,e). For this reason, the years 2006—a transition from La Niña to El Niño—and 2010—a transition from El Niño to La Niña—were selected. In both cases, the contour maps resulted in years of rainfall anomalies, characteristic of transition, i.e., with positive rainfall anomalies in the Altiplano and negative ones in the coast of Nayarit, as occurred in 2006, or with above rainfall anomalies in both regions, as occurred in 2010. We also selected 1999 because it was a year of rainfall anomalies characteristic of La Niña years, i.e., positive anomalies in Nayarit coast and negative anomalies in the Altiplano (Figure 2c).

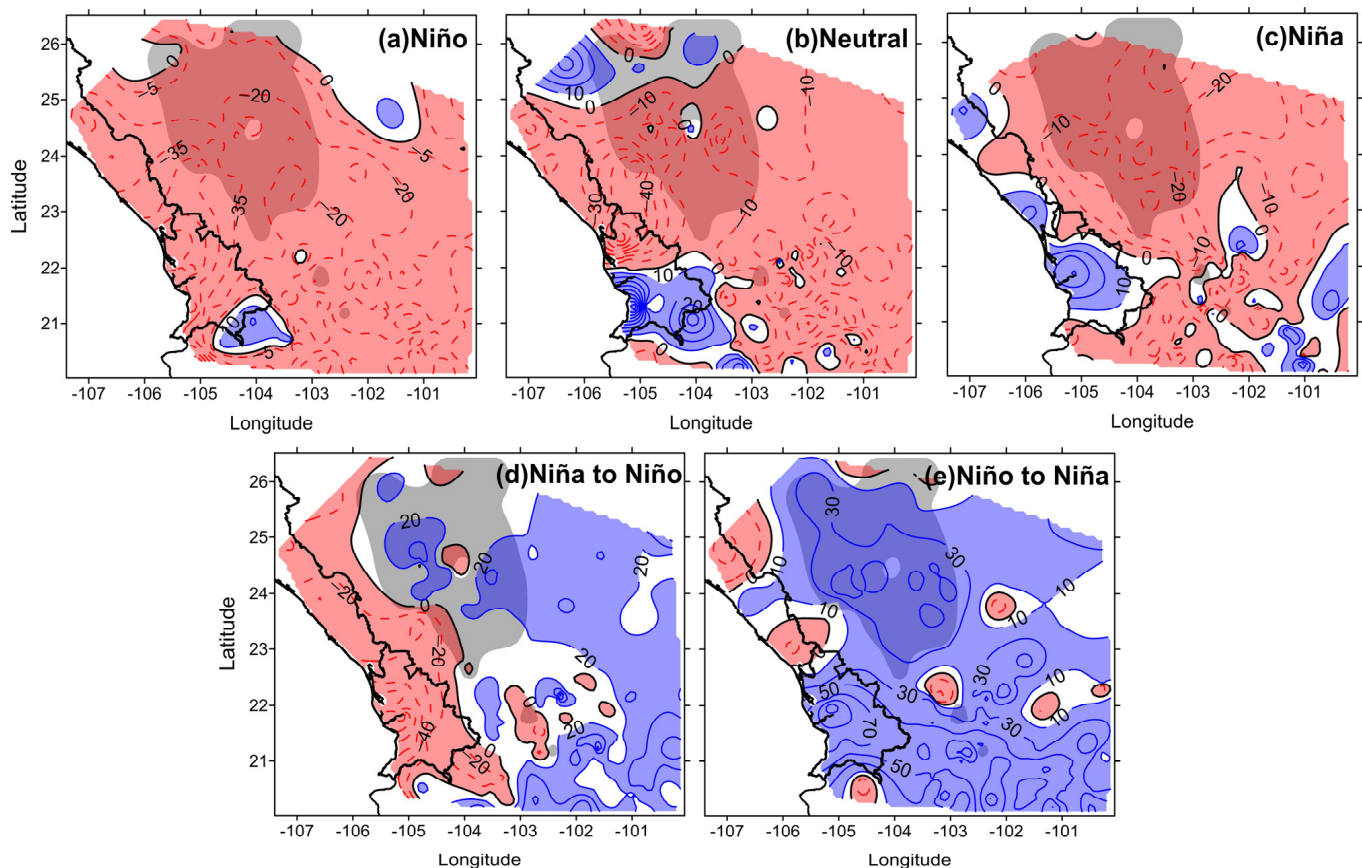


Figure 2. Average contours of summer precipitation anomalies (in mm: July, August, September) for (a) 1982, 1987, 1997—El Niño years; (b) 1979, 1980, 1993—neutral; and (c) 1971, 1974, 2011—La Niña years; (d) 1976, 2009—transition years from La Niña to El Niño; (e) 1973, 1983—transition years from El Niño to La Niña La Niña. Blue (red) contours show positive (negative) anomalies. The shaded area represents the Mexican Altiplano.

Finally, 1998 was selected—a year of transition from El Niño to La Niña—and 2005, neutral, because both years were atypical. In the former, the Altiplano is dry and the Nayarit coast is rainy, while the average map of such a transition shows that above-average rainfall anomalies are characteristic in both regions (Figure 2a). In 1998, a prolonged

drought began in northern Mexico that lasted until 2001; 2005 was a transition year from normal to dry conditions in terms of rainfall anomalies [28]. Both regions are dry, while the average map shows that under neutral conditions, the Nayarit coast is wet and the Altiplano dry (Figure 2b), which raises interest regarding elucidating the origin of those deviations. It should also be noted that under certain atmospheric conditions, a see-saw rainfall behavior can be observed between the regions, as proposed in another study [23]. The importance of this analysis resides in finding a possible mechanism of atmospheric coupling response that connects both regions. Thus, when dry conditions on the coast of Nayarit prevail, conditions that are more humid are expected in the Altiplano and vice versa [23].

All simulations were initialized at 0000 UTC 01 July and ended at 1800 UTC 30 September for each year, and a six-hourly output was available. Selected fields of the WRF simulations were compared with land observations from three weather stations located in the 5 km resolution domain.

2.5. Satellite Imagery

To determine the distribution of cloud cover, a dataset from the Geostationary Operational Environmental Satellite (GOES) was used, centered over the Pacific Ocean at 135° W. The dataset includes imagery from the infrared (10.7 μm) channel with a 4×8 km spatial resolution, which is capable of measuring cloud-top temperature and thus provides an estimate of the vertical convection development as a proxy of precipitation. The imagery is courtesy of the Unidata Program Center at the University Corporation for Atmospheric Research and the Space Science and Engineering Center of the University of Wisconsin-Madison. During the warm season, in the study area, cloud tops colder than -38 °C generally delineate deep clouds in convective systems with tops above 10 km (e.g., Farfán et al., 2021). Convection was analyzed at night (0300 UTC, 2100 LT) and midnight (0600 UTC) since these are times during which deep convection is well-defined over mainland Mexico in a region located between the western foothills of the Sierra Madre Occidental and the Gulf of California coastline.

3. Results

3.1. Precipitation Anomalies

Figures 3 and 4 show contours of summer rainfall anomalies from 1998, 2005, and 1999 (Figure 3), and 2006 and 2010 (Figure 4) based on observations, and correspond to 5 km D03 WRF domain. The configuration of rainfall anomalies in 1998 and 1999 were opposite in phase between the Nayarit coast and Altiplano, that is, above-normal rainfall in Nayarit and a deficit in the Altiplano (Figure 3a,c). In 2005, under neutral ENSO conditions (Figure 3b), rainfall deficits were mostly in both regions, while in central Sinaloa, a core of positive anomalies is evident.

In the JAS of 2006 (Figure 4a), below-average rainfall conditions dominate in Nayarit, which contrasts with the dominance of above-average rainfall in the Altiplano. Additionally, a core of positive rainfall anomalies is present in central Sinaloa. On the other hand, in 2010, positive rainfall anomalies occurred in both regions, but with deficits in central Sinaloa (Figure 4b).

3.2. Atmospheric Moisture Flux

To investigate the moisture transport mechanisms from the ocean to the Altiplano, Figures 5 and 6 show WRF wind vectors at lower (1000 hPa), middle (500 hPa), and upper (200 hPa) levels.

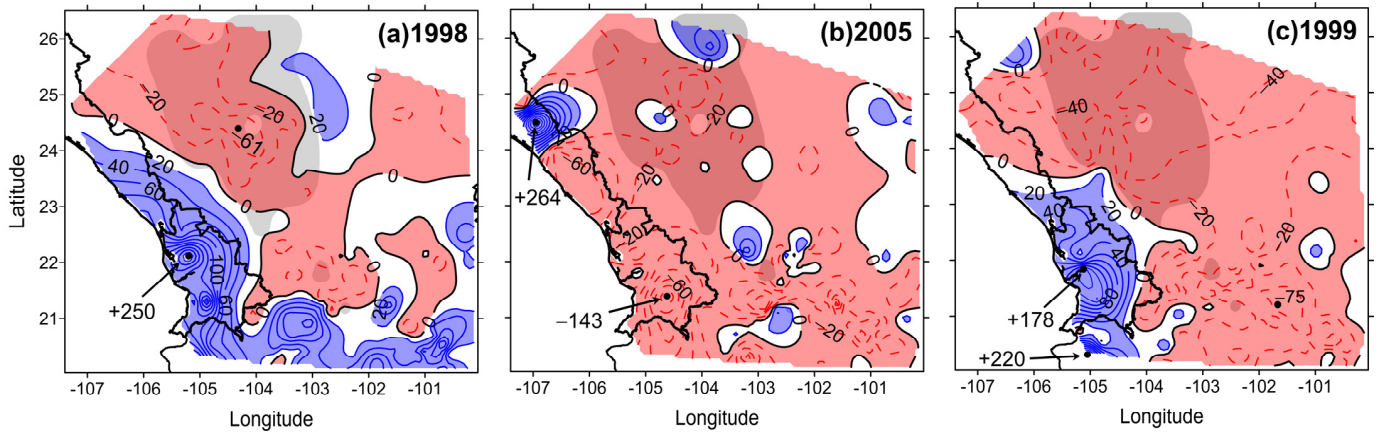


Figure 3. Contours of rainfall anomalies (in mm) during the summer in July, August, September (JAS) for: (a) 1998 (transition from El Niño to La Niña conditions); (b) 2005 (neutral); and (c) 1999 (La Niña). Blue (red) contours show positive (negative) anomalies. The shaded area represents the Mexican Altiplano. Thick polygons represent the states of Sinaloa and Nayarit, Mexico.

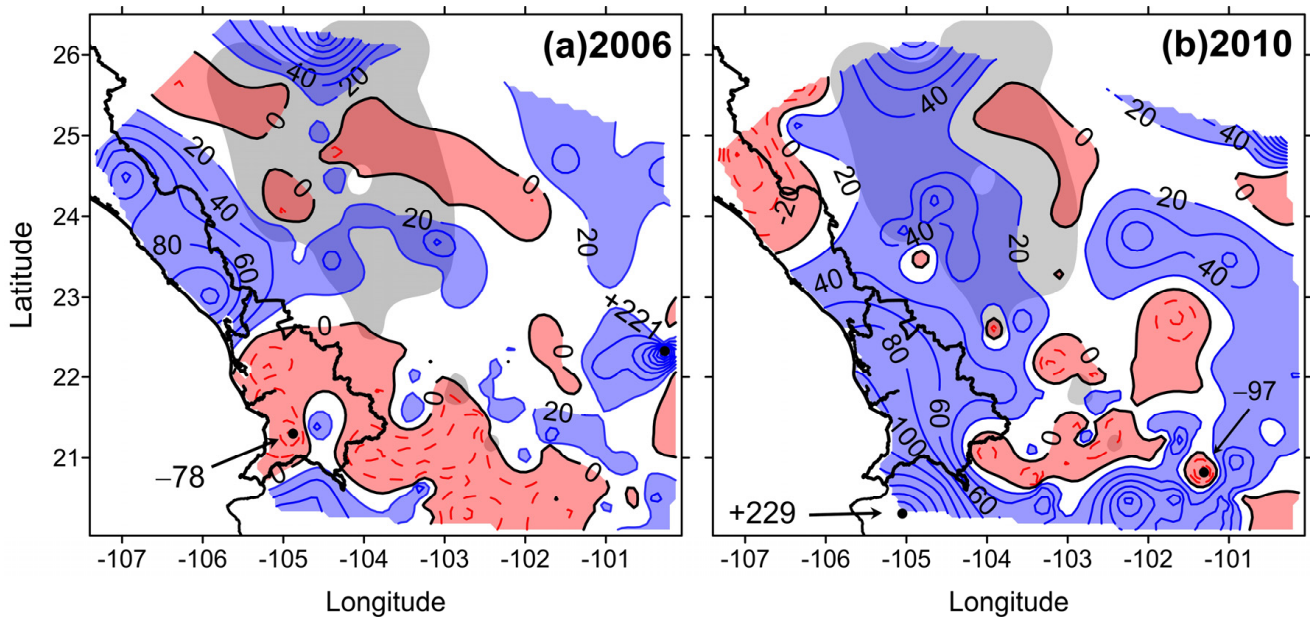


Figure 4. Contours of rainfall anomalies (in mm) during the summer July, August, September (JAS) for: (a) 2006 and (b) 2010. Blue (red) contours show positive (negative) anomalies. The shaded area shows the region of the Mexican Altiplano. Thick polygons represent the states of Sinaloa and Nayarit, Mexico.

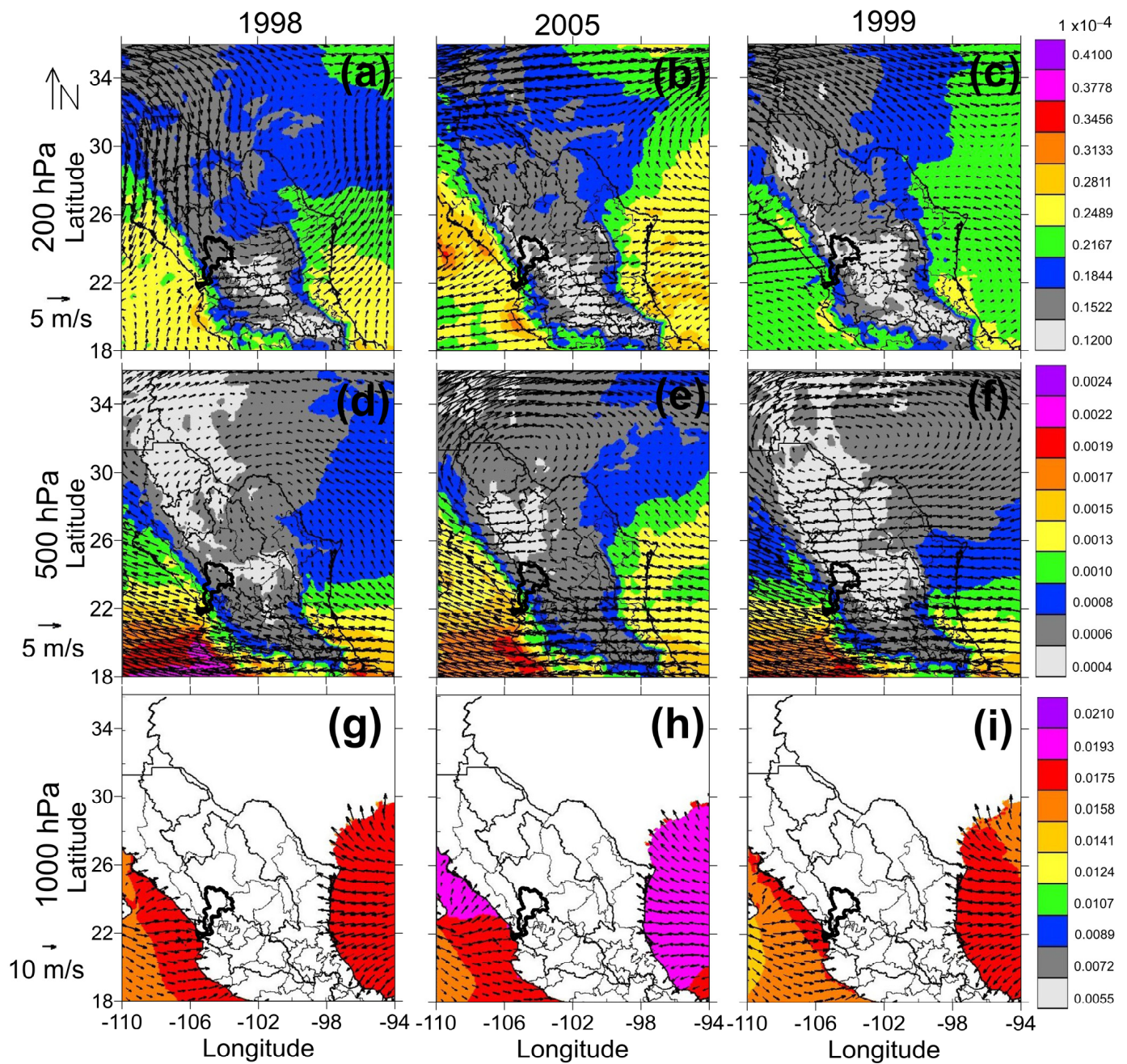


Figure 5. Mean summer July, August, September (JAS) wind vectors ($\text{m}\cdot\text{s}^{-1}$) and water vapor mixing ratio ($\text{kg}\cdot\text{kg}^{-1}$) calculated via weather research and forecasting (WRF 15 km, D02) at three levels for: 1998 (a,d,g, year of transition from El Niño to La Niña); 2005 (b,e,h, neutral); and 1999 (c,f,i, La Niña). The San Pedro-Mezquital River Basin (SPM-RB) polygon is given by the thin line.

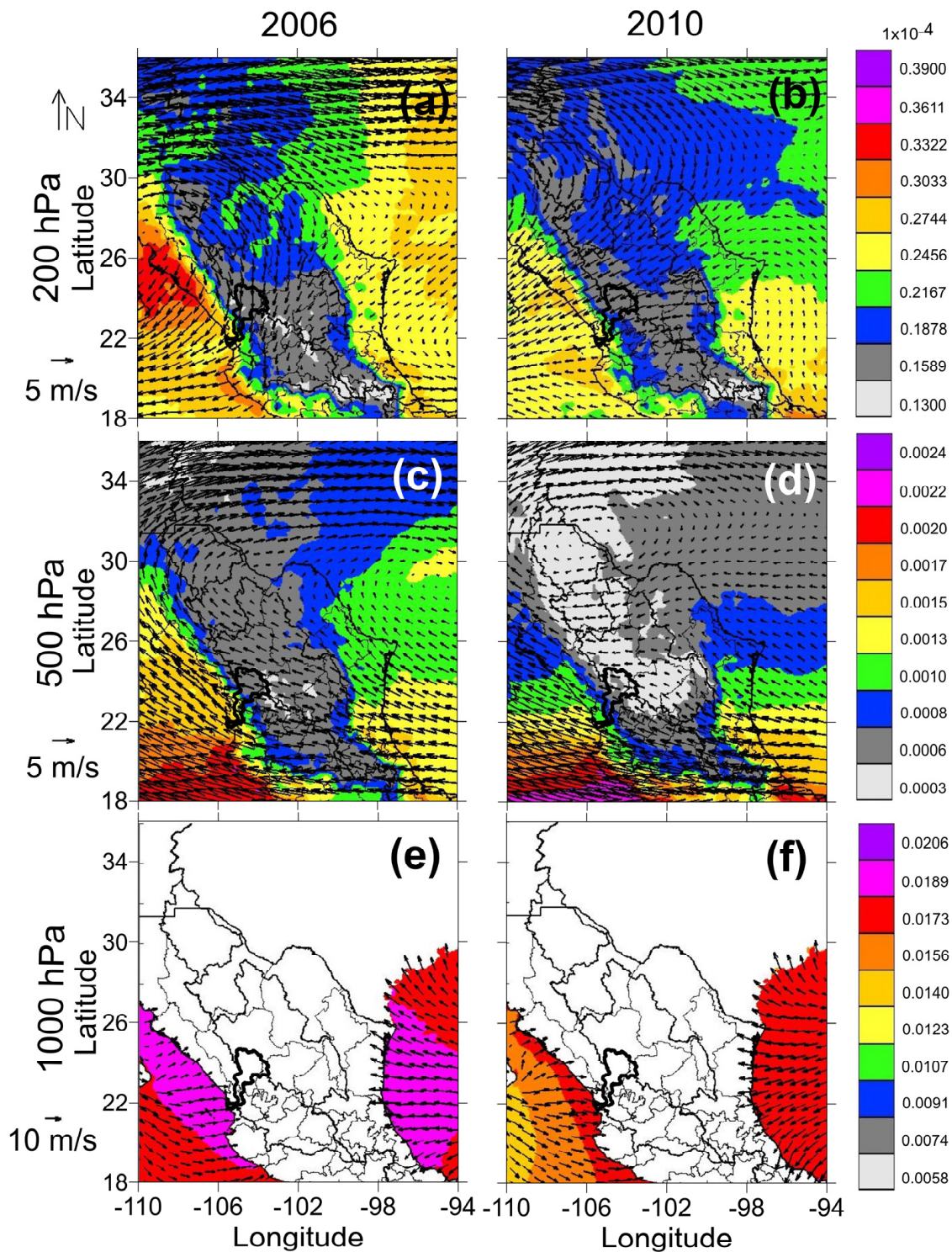


Figure 6. Mean summer July, August, September (JAS) wind vectors ($\text{m} \cdot \text{s}^{-1}$) and water vapor mixing ratio ($\text{kg} \cdot \text{kg}^{-1}$) calculated via weather research and forecasting (WRF 15 km, D02) at three levels for: 2006 (a,c,d, year of transition from La Niña to El Niño) and 2010 (b,d,f, year of transition from El Niño to La Niña). The San Pedro-Mezquital River Basin (SPM-RB) polygon is given by the thin line.

From July to September, under transition (Figure 5g), neutral (Figure 5h) and La Niña conditions (Figure 5i) at lower levels, the winds produce a very similar circulation pattern in the three cases, with winds moving inland from the coast. Winds coming from the coast converge with the continental wind on a trajectory from NW to SE just over the

SPM-RB (see middle panels in Figure 5d–f). This circulation coincides with the mechanisms proposed in a previous work [23] regarding moisture fluxes.

At higher levels, winds change significantly. In 1998, for example, the western branch of a cyclonic circulation in Northern Mexico was dominated by northerly winds that converge with southwestern winds in the region of the SPM-RB (Figure 5a). As previously mentioned, westerly winds dominate along the coast of Nayarit and converge with northerly winds on the continent just on the Altiplano. In both trajectories, winds that cross the basin are weak, and those coming from the north might be dry. A decreasing gradient of water vapor mixing ratio from the land mass to the coast at 200 hPa and 500 hPa is consistent with less rainfall in the Altiplano and above-average anomalies in the coast as described in a previous work [23]. In this case, the see-saw pattern can be determined via moisture fluxes, either at high levels of the troposphere or via flux displacement towards the northwest (Sinaloa), only in the region of the monsoon core [2,5,35–37].

In 2005 (Figure 5b), two circulation patterns at 200 hPa are dominant—an anticyclonic circulation over Northwestern Mexico and easterly winds over Mexico. Under these conditions, the prevailing northeastern winds flow over the SPM-RB, reducing the water vapor mixing ratio at this level. At 500 hPa, the anticyclonic circulation positioned north of Mexico maintains easterly winds over the Altiplano and the mixing ratios are reduced, which is consistent with rainfall deficits over the Altiplano and along the Nayarit coast in 2005. In 1999 (Figure 5c), an anticyclonic circulation over the Baja California Peninsula covered a larger area than in 2005. This circulation favored a dominant continental flow from the north that crossed the basin of the SPM-RB, which has been described as the main driver of exceptional drought during La Niña over the Altiplano [7,19,34,38].

Relative to 2006 (a mostly dry season) and 2010 (wet), the position of the anticyclonic circulation at the middle and upper levels of the troposphere was further north in 2010 than in 2006. This situation allowed more moisture transport into the Altiplano and the coast of Nayarit from the Gulf of Mexico, which resulted in positive anomalies in both regions in 2010. In 2006, the anticyclone—whose center was positioned to the south of the Gulf of California—reduced the water vapor mixing ratio at 200 hPa over the coast of Nayarit. Low values of water vapor mixing ratio are also observed at 500 hPa. The reduced water vapor at the middle and upper levels implies that moisture is not enough for rainfall generation, causing negative rainfall anomalies in Nayarit in 2006. However, enhanced water vapor along the coasts of Nayarit and Sinaloa and the inland southwestern flow at 1000 hPa enable moisture advection from the coast into the mainland. These conditions, in combination with the southeastern flow at 500 hPa, result in increased convection in the Altiplano and explain the above-average precipitation in 2006.

The core of positive (negative) rainfall anomalies in 2006 (2010) in central Sinaloa deserves attention because it is a region of intense agricultural activity and wet-dry changes can significantly affect food production. Figure 6a shows that the wind field from the coast into the mainland at low levels and with the anticyclone positioned in Southcentral GC at upper levels of the troposphere are related to enhanced water vapor mixing ratio (in 2006) in central Sinaloa. This configuration is consistent with the above-average rainfall anomalies. Unlike in 2006, the center of upper-level anticyclonic circulation is positioned further north in 2010 (Figure 6b). In particular, when the wind flow crosses the SMOc, it loses some moisture over the Altiplano, resulting in rainfall deficit over central Sinaloa.

Table 2 summarizes the results found between the atmospheric flow pattern and precipitation conditions for different ENSO conditions between the coast and the Altiplano.

Table 2. Oceanic-atmospheric conditions of the different years of study.

Year	ENSO-Conditions	Weather Pattern	Rainfall-Conditions
1998	Transition from El Niño to La Niña	Cyclonic circulation in Northern Mexico at 200 hPa. Westerly inland flow at 1000 hPa.	Coast: wet Altiplano: dry

Table 2. Cont.

Year	ENSO-Conditions	Weather Pattern	Rainfall-Conditions
1999	La Niña	Anticyclonic circulation in Northwestern Mexico at 200 hPa. Westerly flow at 1000 hPa.	Coast: wet Altiplano: dry
2005	Neutral	Two anticyclone circulations, one centered in Northwest Mexico and the other one in the Northern Gulf of Mexico at upper levels. Westerly flow at 1000 hPa with higher humidity on the Sinaloa Coast.	Coast: dry Altiplano: dry
2006	Transition from La Niña to El Niño	Anticyclone centered south of the Gulf of California at 200 hPa. Southeast flow at 500 hPa.	Coast: dry Altiplano: wet
2010	Transition from El Niño to La Niña	Anticyclonic circulation positioned further to the north at upper and middle level. Westerly inland flow at 1000 hPa.	Coast: wet Altiplano: wet

3.3. Vertically Integrated Moisture Flux

The moisture flux variations determine the precipitation anomalies in the Altiplano that yield periods of drought or abundant rainfall [19]. To understand more about atmospheric conditions related to dry-wet changes, the vertically integrated moisture flux convergence (VIMFC) was calculated for all the cases. Figure 7 shows the sequence of the VIMFC for the transition from El Niño to La Niña (Figure 7a), neutral conditions (Figure 7b), and La Niña (Figure 7c).

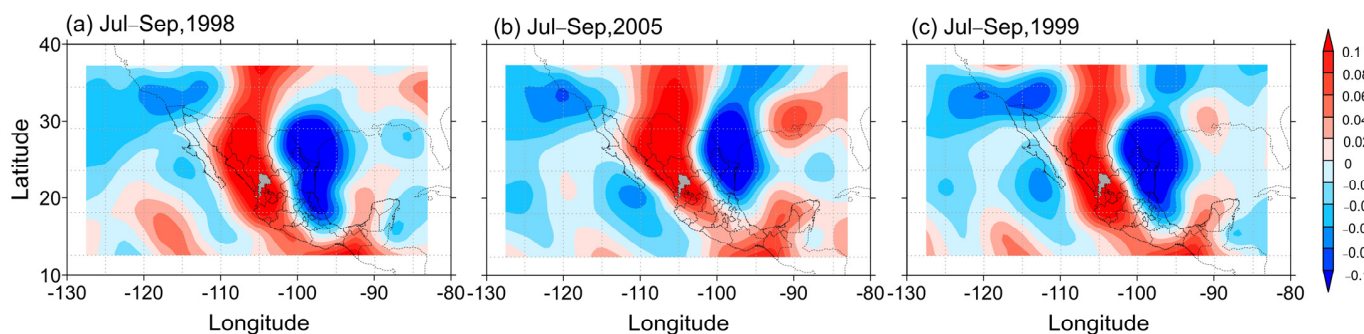


Figure 7. Vertically integrated moisture flux convergence ($\text{g}\cdot\text{kg}^{-1}\cdot\text{s}^{-1}$) from 1000 to 300 hPa based on NARR data for: (a) El Niño to La Niña Transition; (b) Neutral conditions; and (c) La Niña conditions. The polygon with shading area represents the basin of the San Pedro-Mezquital River (SPM-RB).

In the sequence of the years with El Niño/La Niña effect, i.e., in the transition phases from positive (Niño) to negative (La Niña) (Figure 7a,c), the moisture convergence zones extend towards Northwestern Mexico, decreasing in coverage over the Gulf of California for the cold phase. This result agrees with previous works, where ENSO is related to years of dry or wet summers [2,39]. On the other hand, under neutral conditions, the maximum convergence was located forward to the northwest of the SPM-RB (Figure 7b), a configuration that is also observed in 2006 (Figure 8a). In this case, a decreasing gradient in humidity was observed toward the Nayarit region, which contrasted with a slight increase in the Altiplano region. During the conditions of high moisture convergence just off coastal Nayarit (Figure 8b), an increasing gradient toward the Altiplano can be observed.

Figure 9 shows the average frequency of cloud tops from July to September for 2006 and 2010; their difference is based on a threshold of brightness temperature of $-38\text{ }^\circ\text{C}$ (10.5 km above sea level). Note that compared to 2010, an elongated area with a higher frequency of cloud tops from central Sinaloa to southern Sonora was evident in 2006. This result is reinforced by the negative anomalies observed and is consistent with the core of above- (below-) average rainfall anomalies observed in central Sinaloa in 2006 (2010). Likewise, in coastal Nayarit a lower frequency of cloud tops was observed in 2006 compared to 2010, which is consistent with below- (above-) average precipitation (see Figure 4) and

positive anomalies. Finally, anomaly contours and near-zero frequency of cloud tops in the Altiplano indicate that 2006 and 2010 were both years of above-average rainfall anomalies, as shown in Figure 4.

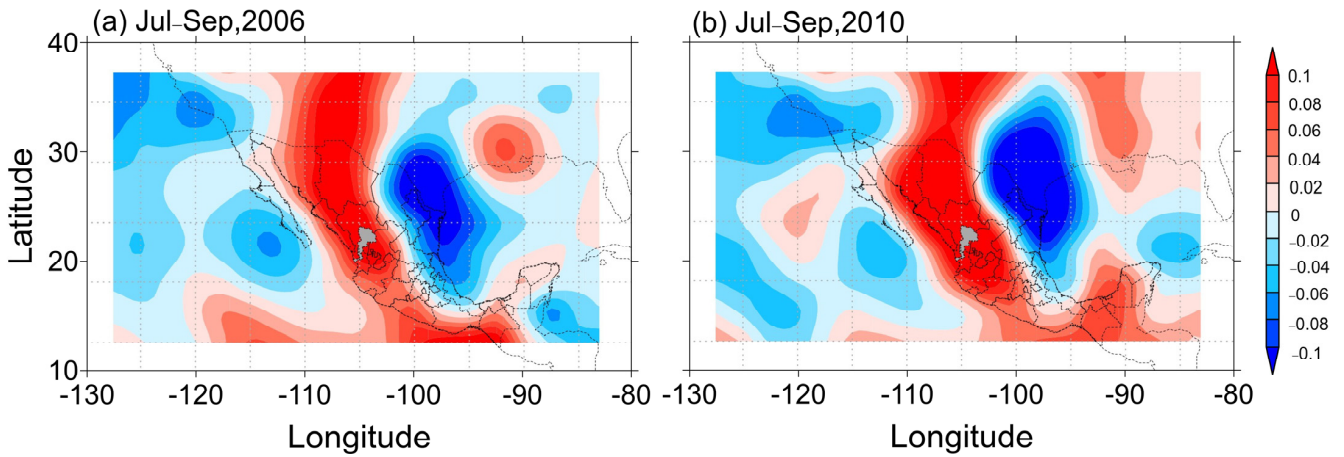


Figure 8. Vertically integrated moisture flux convergence ($\text{g}\cdot\text{kg}^{-1}\cdot\text{s}^{-1}$) from 1000 to 300 hPa base on NARR data for: (a) the dry summer of 2006 and (b) the wet summer of 2010 in Nayarit, Mexico. The polygon with shading area represents the basin of the San Pedro-Mezquital River (SPM-RB).

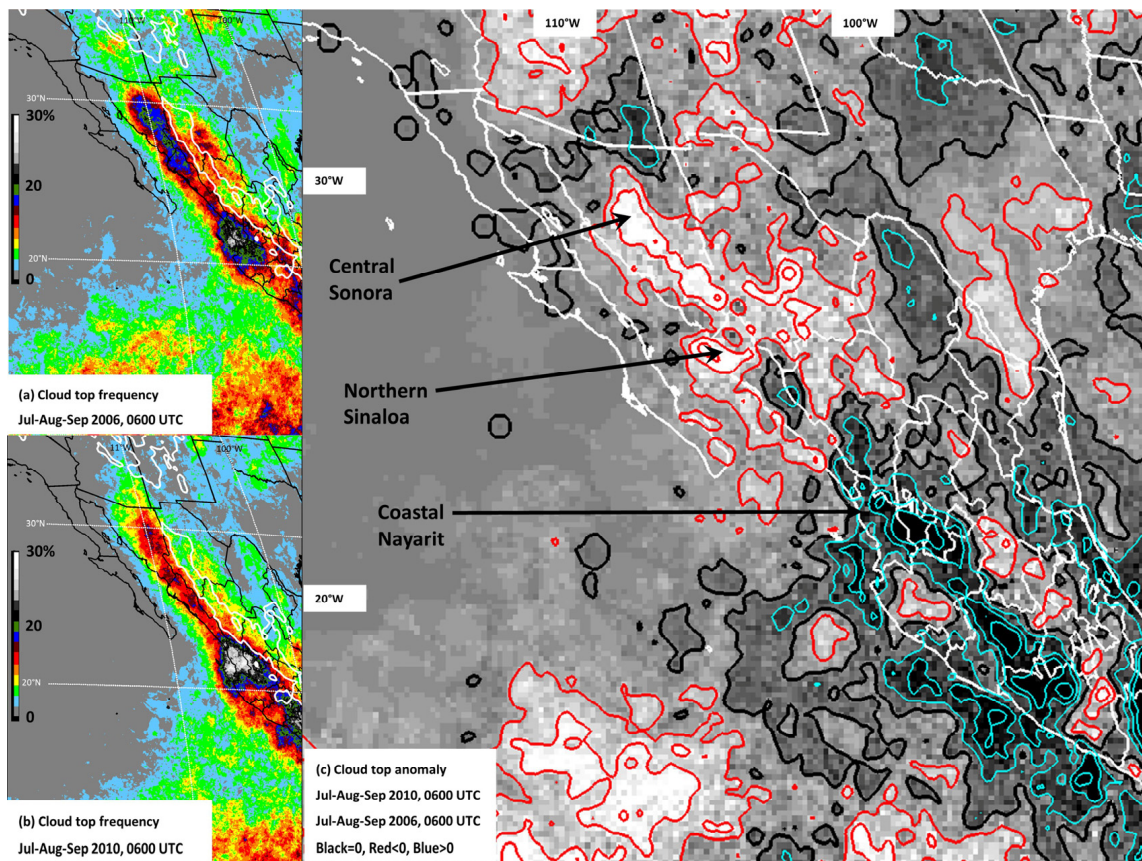


Figure 9. Frequency (%) of cloud tops that reached at least $-38\text{ }^{\circ}\text{C}$ in the infrared imagery from the geostationary operational environmental satellite (GOES) infrared imagery at 0600 UTC. Average conditions from July to September 2006 are in the (a) upper left panel, while the same period from 2010 is in the (b) lower left panel. Anomalies (difference from 2010 minus 2006) are in the (c) right panel; positive (negative) contours are displayed in blue (red) with 20% intervals.

4. Discussion

The analyses of years with intense drought and those with positive rainfall anomalies show how consistently moisture fluxes display large areas of divergence over central Mexico into the Southeastern United States. This situation occurs in response to the high pressure in the Southwestern United States and the contrast between the sea and the continent [40,41]. During periods of more intense drought, two high-pressure cells are observed, generating an anticyclonic circulation in the middle levels (500 hPa) towards the Northeastern Pacific and cold and dry flows on the western coast of North America and Mexico [19,40]. These features have been related to variations in the Eastern Pacific SST [34,39,41], although little has been studied about the effects of the continental contribution on water recycling [40,42].

On the other hand, variations of the moisture fluxes between the opposite, in phase years 2006 (mostly dry) and 2010 (wet), are less strong at the middle and high levels than at lower levels (Figure 6). In Western Mexico, a moisture transport mechanism from the Eastern Pacific region has been previously described [35]. In fact, part of the moisture sources for this region are controlled by the extension of the ITCZ from the tropical Pacific toward the monsoon zone in the Gulf of California [11,39,42–45].

In humid years, such as 2006, an anticyclonic circulation at middle and high levels favors moisture transport to central Mexico (Figure 6a). At low levels, the flows into the continent are mainly from the Eastern Pacific and the Gulf of California. Recently, the possibility of moisture transport from the Gulf of Mexico at high levels occurs mainly at the beginning of summer [42]. Additionally, an important contribution of continental water recycling through evaporation has been identified, which can be a more important source of rainfall in years where large-scale moisture advection is reduced [35].

The analyses of 2006 and 2010 are interesting because the moisture fluxes are expected to move through the basin lowlands, just over the coast of Nayarit towards the Altiplano, explaining the mechanism of humidity transport at middle and low levels. Specifically, under the conditions of positive rainfall anomalies in Nayarit, a rainfall increase in the Altiplano would be expected, as in the case in 2010. That is, when moisture flux patterns dominate from the Nayarit coastal region to the Altiplano, the anomaly is mostly positive in both regions. In 2006, an orographic rain effect determined less precipitation in Nayarit and more in the Altiplano [23]. These conditions are related to a decrease in precipitation over the monsoon core [39].

In general terms, the periods July–September 2005 (Figure 7b) and 2006 (Figure 8a) were under ENSO neutral conditions when the convergence peak towards North–Northwestern Mexico favored the Altiplano region with above-normal rainfall in 2006 but affected both the coast of Nayarit and the Altiplano regions with below-normal rainfall in 2005. These results agree with those of other authors with respect to moisture flux convergence [35,42]. The Eastern Pacific Ocean (including the Gulf of California) is the main source of humidity for the continental regions of Northern Mexico and Southwestern United States [34,44]. The moisture transport is controlled by circulation at surface levels that intensify El Niño in the positive phases [2,34,45] but decrease in the negative ones [2,3,12], which, in turn, favors fluxes from the regions, such as the Gulf of Mexico or at medium and high levels [38]. As discussed by Bracken et al. [39], a greater effect of ENSO is observed on the pathway of moisture rather than on the source; consequently, ENSO could increase middle-level fluxes under such conditions.

5. Conclusions

In the Altiplano of Central Mexico, an important region for the national economy, rainfall is the main input for agricultural activities. Persistent or severe droughts cause a high impact at the local and national level. Different scenarios were studied using the Oceanic Niño Index and precipitation anomaly. In transition phases (El Niño to La Niña or from La Niña to El Niño), a greater impact is observed on summer precipitation in the Altiplano, which increases when the transition occurs under constructive (destructive) PDO and AMO signals [4].

Moisture generated in the Eastern Pacific enters the continent, affecting the states of Nayarit, Durango, and Zacatecas. Between the coast of Nayarit and the Mexican Altiplano, a see-saw pattern can be observed in summer rainfall anomalies [23]. In other words, drought conditions in the Altiplano tend to occur with humid conditions on the coast of Nayarit and vice versa, although an increase or decrease in summer precipitation in central Sinaloa is evident to the south of the monsoon core. This connection mechanism between Nayarit and the Altiplano is partly explained by moisture fluxes at lower levels. Circulation towards the Altiplano is controlled by the SST conditions of the Eastern Pacific and also by an anticyclonic circulation at upper levels in the Northern United States. Additionally, this circulation yields a dry flow towards the highlands from the north–northeastern areas, causing droughts. Moisture convergence at lower levels in the Eastern Pacific on the western coast of Mexico—in combination with the divergence at upper levels—favors moisture transport near the coast, which generates a positive precipitation anomaly in the coastal region.

Although the Gulf of Mexico is a source of moisture for the Altiplano [42], the present study has revealed that the main source of moisture is the Eastern Pacific, including the Gulf of California. The correspondence between these two regions, connected by the San Pedro-Mezquital River Basin, indicates that precipitation is favored by the occurrence of a southerly flow that drags the low-level humidity from the Pacific inland mainly through the canyons of the San Pedro-Mezquital River system. The WRF simulations confirmed that the atmospheric response on the Altiplano changes under different ENSO conditions by strengthening or weakening convective activity. The most favorable scenario for rainfall production in the Altiplano occurred during the transition years from El Niño to La Niña and vice versa. This result was unexpected since Vega-Camarena et al. [19] reported that the transition from an El Niño to La Niña combined with a positive PDO phase and negative AMO phase resulted in moderate drought in the Altiplano. However, if such a transition occurs when the PDO and AMO are both in negative phase (as in 1973) or PDO is neutral and AMO is in positive phase (as in 2010), the conditions in the Altiplano are found to be above-average rainfall. Similarly, according to Vega-Camarena et al. [19], the transition from La Niña to El Niño, in combination with negative phases of PDO and AMO, resulted in moderate drought in the Altiplano. However, if such a transition occurs when the PDO is in the negative phase and the AMO is in the positive phase (as in 2009) or PDO is neutral and AMO is in positive phase (as in 2006), the conditions in the Altiplano are found to be above-average rainfall. These results indicate that rainfall production in the Altiplano depends not only on the ENSO phase but also on the phase combination between the PDO and AMO. Nevertheless, further studies are necessary to elucidate the link observed between central Sinaloa, coastal Nayarit and the Altiplano.

Author Contributions: Conceptualization, J.P.V.-C. and L.B.-C.; methodology, J.P.V.-C., L.B.-C. and L.F.P.-M.; validation, J.P.V.-C., L.B.-C. and L.M.F.; formal analysis, J.P.V.-C., L.B.-C. and L.F.P.-M.; investigation, J.P.V.-C., L.B.-C. and L.F.P.-M.; writing—original draft preparation, J.P.V.-C. and L.B.-C.; writing—review and editing, L.B.-C., L.F.P.-M. and L.M.F. All authors have read and agreed to the published version of the manuscript.

Funding: This project was supported by the Centro de Investigaciones Biológicas del Noroeste (CIBNOR), México (grant PLAYCO 10043) and REDESCLIM-CONACYT (Consejo Nacional de Ciencia y Tecnología, México) (grant 254533). J.P.V.-C. is the recipient of a postdoctoral fellowship from CONACYT (grant 376783).

Institutional Review Board Statement: Not applicable.

Informed Consent Statement: Not applicable.

Data Availability Statement: Rainfall datasets used in the analysis are from Servicio Meteorológico Nacional, Mexico “<https://smn.conagua.gob.mx/es/climatologia/informacion-climatologica/informacion-estadistica-climatologica> (accessed on 30 November 2022)”. The weather research and forecasting (WRF) version 4 is available for downloading at “<https://esrl.noaa.gov/gsd/wrfportal/> (accessed on 10 January 2023)”. The North American Regional Reanalysis (NARR) data are available from

“<https://www.esrl.noaa.gov/psd/data> (accessed on 12 January 2023)”. The NOAA Climate Prediction Center “<https://www.cpc.ncep.noaa.gov/> (accessed on 13 February 2023)”, provides ONI. Other indices (i.e., the Multivariate ENSO Index or MEI V2; NOAA Physical Sciences Laboratory are available at: “<https://psl.noaa.gov/data/climateindices/list/index.html> (accessed on 13 February 2023)”).

Acknowledgments: The authors are grateful to Julio Egrén Félix Domínguez from CIBNOR Spatial Modeling and Remote Sensing Laboratory for technical support in obtaining the SMN data; to Diana Fischer for English Edition.

Conflicts of Interest: The authors declare no conflict of interest.

References

1. Cavazos, T. Large-scale circulation anomalies conducive to extreme precipitation events and derivation of daily rainfall in northeastern Mexico and southeastern Texas. *J. Clim.* **1999**, *12*, 1506–1523. [[CrossRef](#)]
2. Higgins, R.W.; Douglas, A.; Hahmann, A.N.; Berbery, E.H.; Gutzler, D.; Shuttleworth, W.J.; Stensrud, D.; Amador, J.A.; Carbone, R.; Lobato-Sánchez, R.; et al. Progress in Pan American climate research: The North American monsoon system. *Atmosfera* **2003**, *16*, 29–65.
3. Méndez, M.; Magaña, V. Regional aspects of prolonged meteorological droughts over Mexico and Central America. *J. Clim.* **2010**, *23*, 1175–1188. [[CrossRef](#)]
4. Pavia, E.G.; Graef, F.; Reyes, J. PDO–ENSO effects in the climate of Mexico. *J. Clim.* **2006**, *19*, 6433–6438. [[CrossRef](#)]
5. Douglas, M.W.; Maddox, R.A.; Howard, K.; Reyes, S. The Mexican Monsoon. *J. Clim.* **1993**, *6*, 1665–1677. [[CrossRef](#)]
6. Magaña, V.O.; Vázquez, J.L.; Pérez, J.L.; Pérez, J.B. Impact of El Niño on precipitation in Mexico. *Geofís. Int.* **2003**, *42*, 313–330. [[CrossRef](#)]
7. Clarke, A.J. *An Introduction to the Dynamics of El Niño and the Southern Oscillation*, 1st ed.; Elsevier: Amsterdam, The Netherlands, 2008.
8. Englehart, P.J.; Douglas, A.V. The role of eastern North Pacific tropical storms in the rainfall climatology of western Mexico. *Int. J. Climatol.* **2001**, *21*, 1357–1370. [[CrossRef](#)]
9. Ropelewski, C.F.; Halpert, M.S. Quantifying southern oscillation-precipitation relationships. *J. Clim.* **1996**, *9*, 1043–1059. [[CrossRef](#)]
10. Seager, R.; Kushnir, Y.; Herweijer, C.; Naik, N.; Velez, J. Modeling of tropical forcing of persistent droughts and pluvials over western North America: 1856–2000. *J. Clim.* **2005**, *18*, 4065–4088. [[CrossRef](#)]
11. Castro, C.L.; McKee, T.B.; Pielke, R.A. The relationship of the North American monsoon to tropical and North Pacific Sea surface temperatures as revealed by observational analyses. *J. Clim.* **2001**, *14*, 4449–4473. [[CrossRef](#)]
12. Seager, R.; Ting, M.; Davis, M.; Cane, M.; Naik, N.; Nakamura, J.; Stahle, D.W. Mexican drought: An observational modeling and tree ring study of variability and climate change. *Atmosfera* **2009**, *22*, 1–31.
13. Reyes, S.; Mejía-Trejo, A. Tropical perturbations in the eastern Pacific and the precipitation field over northwestern Mexico in relation to the ENSO phenomenon. *Int. J. Climatol.* **1991**, *11*, 515–528. [[CrossRef](#)]
14. Zolotokrylin, N.A.; Titkova, T.B.; Brito-Castillo, L. Wet and dry patterns associated with ENSO events in the Sonoran Desert from 2000–2015. *J. Arid. Environ.* **2016**, *134*, 21–32. [[CrossRef](#)]
15. Cid-Serrano, L.; Ramírez, S.M.; Alfaro, E.J.; Enfield, D.B. Analysis of the Latin American west coast rainfall predictability using an ENSO index. *Atmosfera* **2015**, *28*, 191–203. [[CrossRef](#)]
16. Newman, M.; Alexander, M.A.; Ault, T.R.; Cobb, K.M.; Deser, C.; Di Lorenzo, E.; Mantua, N.J.; Miller, A.J.; Minobe, S.; Nakamura, H.; et al. The Pacific Decadal Oscillation, Revisited. *J. Clim.* **2016**, *29*, 4399–4426. [[CrossRef](#)]
17. Wang, S.; Huang, J.; He, Y.; Guan, Y. Combined effects of the Pacific Decadal Oscillation and El Niño–Southern Oscillation on Global Land Dry–Wet Changes. *Sci. Rep.* **2014**, *4*, 6651. [[CrossRef](#)]
18. Stahle, D.W.; Cook, E.R.; Burnette, D.J.; Villanueva, J.; Cerano, J.; Burns, J.N.; Griffin, D.; Cook, B.I.; Auña, R.; Torbenson, M.C.A.; et al. The Mexican drought atlas: Tree-ring reconstructions of the soil moisture balance during the late pre-Hispanic, colonial, and modern eras. *Quat. Sci. Rev.* **2016**, *149*, 34–60. [[CrossRef](#)]
19. Vega-Camarena, J.P.; Brito-Castillo, L.; Farfán, L.M.; Gochis, D.J.; Pineda-Martínez, L.F.; Díaz, S.C. Ocean–atmosphere conditions related to severe and persistent droughts in the Mexican Altiplano. *Int. J. Climatol.* **2018**, *38*, 853–866. [[CrossRef](#)]
20. Martínez-Sánchez, J.N.; Cavazos, T. Eastern tropical Pacific hurricane variability and landfalls on Mexican coasts. *Clim. Res.* **2014**, *58*, 221–234. [[CrossRef](#)]
21. Farfán, L.M.; Barrett, B.S.; Raga, G.B.; Delgado, J.J. Characteristics of mesoscale convection over northwestern Mexico, the Gulf of California, and Baja California Peninsula. *Int. J. Climatol.* **2021**, *41*, E1062–E1084. [[CrossRef](#)]
22. Brito-Castillo, L.; Vivoni, E.R.; Gochis, D.J.; Filonov, A.; Tereshchenko, I.; Monzon, C. An anomaly in the occurrence of the month of maximum precipitation distribution in northwest Mexico. *J. Arid. Environ.* **2010**, *74*, 531–539. [[CrossRef](#)]
23. Vega-Camarena, J.P.; Brito-Castillo, L.; Farfán, L.M. Contrasting rainfall behavior between the Pacific coast and the Mexican Altiplano. *Clim. Res.* **2018**, *76*, 225–240. [[CrossRef](#)]
24. Brito-Castillo, L.; Farfán, L.M.; Antemate-Vealisco, G.J. Effect of the Trans-Volcanic Axis on meridional propagation of summer precipitation in western Mexico. *Int. J. Climatol.* **2022**, *42*, 9304–9318. [[CrossRef](#)]
25. Vera, C.; Higgins, W.; Amador, J.; Ambrizzi, R.; Garreaud, R.; Gochis, D.J.; Gutzler, D.; Lettenmaier, D.; Marengo, J.; Mechoso, C.R.; et al. Toward a unified view of the American monsoon systems. *J. Clim.-Spec. Sect.* **2006**, *19*, 4977–5000. [[CrossRef](#)]

26. Servicio Meteorológico Nacional (SMN). Información Estadística Climatológica. Available online: <https://smn.conagua.gob.mx/es/climatologia/informacion-climatologica/informacion-estadistica-climatologica> (accessed on 30 November 2022).
27. Colle, B.A.; Mass, C.F. The 5–9 February 1996 flooding event over the Pacific Northwest: Sensitivity studies and evaluation of the MM5 precipitation forecasts. *Mon. Weather. Rev.* **2000**, *128*, 593–617. [[CrossRef](#)]
28. Fritsch, J.M.; Houze, R.A., Jr.; Adler, R.; Bluestein, H.; Bosart, L.; Brown, J.; Carr, F.; Davis, C.; Johnson, R.H.; Junker, N.; et al. Quantitative precipitation forecasting: Report of the Eighth Prospectus Development Team, U.S. Weather Research Program. *Bull. Am. Meteorol. Soc.* **1998**, *79*, 285–299.
29. Stoelinga, M.T.; Hobbs, P.V.; Mass, C.F.; Locatelli, J.D.; Colle, B.A.; Houze, R.A.; Rangno, A.L.; Bond, N.A.; Smull, B.F.; Rasmussen, R.M.; et al. Improvement of microphysical parameterization through observational verification experiment. *Bull. Am. Meteorol. Soc.* **2003**, *84*, 1807–1826. [[CrossRef](#)]
30. Skamarock, W.C.; Klemp, J.B.; Dudhia, J.; Gill, D.O.; Liu, Z.; Berner, J.; Wang, W.; Powers, J.G.; Duda, M.G.; Barker, D.M.; et al. *A Description of the Advanced Research WRF Model Version 4*; National Center for Atmospheric Research: Boulder, CO, USA, 2019; Volume 145, p. 550.
31. Mesinger, F.; DiMego, G.; Kalnay, E.; Mitchell, K.; Shafran, P.C.; Ebisuzaki, W.; Jović, D.; Woollen, J.; Rogers, E.; Berbery, E.H.; et al. North American Regional Reanalysis. *Bull. Am. Meteorol. Soc.* **2006**, *87*, 43–360. [[CrossRef](#)]
32. Mo, K.C.; Chelliah, M.; Carrera, M.; Higgins, R.W.; Ebisuzaki, W. Atmospheric moisture transport over the United States and Mexico as evaluated from the NCEP Regional Reanalysis. *J. Hydrometeorol.* **2005**, *6*, 710–728. [[CrossRef](#)]
33. SAGARPA (Secretaría de Agricultura, Ganadería, Desarrollo Rural, Pesca y Alimentación). *Base de Datos de PROCAMPO*; Delegación Zacatecas: Zacatecas, Mexico, 2003.
34. Ropelewski, C.F.; Halpert, M.S. North American precipitation and temperature patterns associated with the El Niño/Southern Oscillation (ENSO). *Mon. Weather Rev.* **1986**, *114*, 2352–2362. [[CrossRef](#)]
35. Castro, C.L.; Chang, H.I.; Dominguez, F.; Carrillo, C.; Schemm, J.K.; Juang, H.M.H. Can a regional climate model improve the ability to forecast the North American monsoon? *J. Clim.* **2012**, *25*, 8212–8237. [[CrossRef](#)]
36. Dominguez, F.; Kumar, P.; Vivoni, E.R. Precipitation recycling variability and Ecoclimatological stability—A study using NARR data. Part II: North American monsoon region. *J. Clim.* **2008**, *21*, 5187–5203. [[CrossRef](#)]
37. Turrent, C.; Cavazos, T. Role of the land-sea thermal contrast in the interannual modulation of the North American Monsoon. *Geophys. Res. Lett.* **2009**, *36*, L02808. [[CrossRef](#)]
38. Vicente-Serrano, S.M.; López-Moreno, J.I.; Gimeno, L.; Nieto, R.; Morán-Tejeda, E.; Lorenzo-Lacruz, J.; Azorin-Molina, C. A multiscale global evaluation of the impact of ENSO on droughts. *J. Geophys. Res. Atmos.* **2011**, *116*, D20. [[CrossRef](#)]
39. Cerezo-Mota, R.; Cavazos, T.; Arritt, R.; Torres-Alavez, A.; Sieck, K.; Nikulin, G.; Salinas-Prieto, J.A. CORDEX-NA: Factors inducing dry/wet years on the North American Monsoon region. *Int. J. Climatol.* **2016**, *36*, 824–836. [[CrossRef](#)]
40. Bosilovich, M.G.; Sud, Y.C.; Schubert, S.D.; Walker, G.K. Numerical simulation of the large-scale North American monsoon water sources. *J. Geophys. Res. Atmos.* **2003**, *108*, D16. [[CrossRef](#)]
41. Torres-Alavez, A.; Cavazos, T.; Turrent, C. Land-sea thermal contrast and intensity of the North American monsoon under climate change conditions. *J. Clim.* **2014**, *27*, 4566–4580. [[CrossRef](#)]
42. Jana, S.; Rajagopalan, B.; Alexander, M.A.; Ray, A.J. Understanding the dominant sources and tracks of moisture for summer rainfall in the southwest United States. *J. Geophys. Res. Atmos.* **2018**, *123*, 4850–4870. [[CrossRef](#)]
43. Bracken, C.; Rajagopalan, B.; Alexander, M.; Gangopadhyay, S. Spatial variability of seasonal extreme precipitation in the western United States. *J. Geophys. Res. Atmos.* **2015**, *120*, 4522–4533. [[CrossRef](#)]
44. Wu, M.C.; Schubert, S.D.; Suarez, M.J.; Huang, M.E. An analysis of moisture fluxes into the Gulf of California. *J. Clim.* **2014**, *22*, 2216–2239. [[CrossRef](#)]
45. Zhang, T.; Yang, S.; Jiang, X.; Zhao, P. Seasonal–interannual variation and prediction of wet and dry season rainfall over the maritime continent: Roles of ENSO and monsoon circulation. *J. Clim.* **2016**, *29*, 3675–3695. [[CrossRef](#)]

Disclaimer/Publisher’s Note: The statements, opinions and data contained in all publications are solely those of the individual author(s) and contributor(s) and not of MDPI and/or the editor(s). MDPI and/or the editor(s) disclaim responsibility for any injury to people or property resulting from any ideas, methods, instructions or products referred to in the content.